https://doi.org/10.5194/egusphere-2023-2685
Preprint. Discussion started: 8 January 2024

A Study on the Transformer-CNN Imputation Method for Turbulent Heat Flux Dataset in the Qinghai-Tibet Plateau Grassland

Quanzhe Hou[1], Zhiqiu Gao[1,2], Zexia Duan[3], and Minghui Yu[1]

[1]School of Atmospheric Physics, Nanjing University of Information Science and Technology, Nanjing 210044, China
[2]State Key Laboratory of Atmospheric Boundary Layer Physics and Atmospheric Chemistry, Institute of Atmospheric Physics, Chinese Academy of Sciences, Beijing 100029, China
[3]School of Electrical Engineering, Nantong University, Nantong 226019, China

Correspondence to: Zhiqiu Gao (zgao@nuist.edu.cn)

Abstract. Based on the turbulent heat flux from the third scientific expedition to the Qinghai-Tibet Plateau in 2012, imputation evaluations were conducted using algorithms like Random Forest, Support Vector Machine (SVM), K-Nearest Neighbors (KNN), Gradient Boosting (XGBoost), Long Short-Term Memory (LSTM), Gated Recurrent Unit (GRU), and the Transformer model with deep self-attention mechanism. Results indicated that the Transformer model performed optimally. To further enhance imputation accuracy, a combined model of Transformer and Convolutional Neural Network (CNN), termed as Transformer_CNN, was proposed. Herein, while the Transformer primarily focused on global attention, the convolution operations in the CNN provided the model with local attention. Experimental outcomes revealed that the imputations from Transformer_CNN surpassed the traditional single artificial intelligence model approaches. The coefficient of determination (R^2) reached 0.949 in the sensible heat flux test set and 0.894 in the latent heat flux test set, thereby confirming the applicability of the Transformer_CNN model for data imputation of turbulent heat flux in the Qinghai-Tibet Plateau. Ultimately, the turbulent heat flux observational database from 2007 to 2016 at the station was imputed using the Transformer_CNN model.

1 Introduction

Tibetan land surface processes play a significant role in influencing Asian weather and climate, primarily through the surface-atmosphere exchange of energy, momentum, and CO2 across the atmospheric boundary layer (Zhang et al., 1996; Collatz et al., 2000; Bounoua et al., 2002; Defries et al., 2002; Chen et al., 2003, Gao et al., 2004, Jiao et al., 2023). Surface turbulent heat fluxes, including sensible and latent heat fluxes, are fundamental determinants of local microclimate formation and serve as crucial regulators for vegetation activity (Chapin et al., 2011). With global climate change, the ecosystems and water resources of the Qinghai-Tibet Plateau have undergone significant impacts. Turbulent heat flux data provide key insights to assess these changes and devise countermeasures. Therefore, the long-term continuous observational data of land-atmosphere turbulent heat flux on the Qinghai-Tibet Plateau hold significant value for studying the region's weather and climate (Swinbank and W.C., 1951; Baotian et al., 1996; Zheng et al., 2000; Baldocchi, 2014; Yu Guirui et al., 2017).

https://doi.org/10.5194/egusphere-2023-2685
Preprint. Discussion started: 8 January 2024

As a direct observation technique for turbulent heat flux, the Eddy Covariance (EC) method stands as the primary observational means for the international flux network (FLUXNET) and a plethora of meteorological, ecological, and hydrological observation sites (Shaoying et al., 2020). Initially proposed by Swinbank (Swinbank and W.C., 1951), EC directly measures the turbulent pulsations of various physical quantities based on micrometeorological principles. It calculates flux by evaluating the covariance produced by wind speed pulsations and physical quantity pulsations during atmospheric turbulent motion, thereby measuring heat, mass, and momentum exchanges between the land and the atmosphere. While this method does not rely on assumptions like the near-surface similarity theory, due to observational principles and instrument construction, a series of necessary corrections, quality controls, and quality assurances must be applied to raw data before obtaining final flux calculation results (X et al., 2005). Additionally, given the Tibetan Plateau's geographical location, high altitude, and harsh natural conditions, during continuous observations of material and energy exchanges between the land and atmosphere, data omissions account for 40% to 60% of the total data. This significant omission rate profoundly affects data integrity and accuracy (Falge et al., 2001; X et al., 2005), subsequently influencing its application in climate and weather models (Stull, 1988). Over the past two decades, domestic and international scientists have extensively researched the quality control and assurance of turbulent flux data, forming standardized processing procedures (Papale et al., 2006; Mauder et al., 2008; Wang Shaoying et al., 2009; Wutzler et al., 2018). However, discussions regarding the imputation of missing flux data remain necessary (Foltynova et al., 2020). Rational imputation methods can enhance the integrity of observational data series, facilitating a more accurate understanding of dynamic changing processes and laying the foundation for simulation experiments. In research on energy and material exchanges between terrestrial ecosystems and the atmosphere, the choice of imputation method is paramount. Seasonal changes in ecological processes and soil moisture can influence measurements of turbulent exchanges (Reichstein et al., 2005). Therefore, selecting imputation methods that capture such complexities is crucial.

Currently, researchers have developed dozens of imputation methods, which can be mainly categorized into the following four types: (1) imputation methods based on mean values; (2) non-linear regression methods driven by environmental factors; (3) imputation methods based on artificial neural networks; and (4) imputation methods based on machine learning algorithms (Falge et al., 2001; Hui et al., 2004; Ooba et al., 2006; Moffat et al., 2007; Soloway et al., 2017; Wang et al., 2020). A rational approach to imputing missing flux data serves as a crucial foundation for data integration among stations and flux observation networks and is a key factor in enhancing data comparability (Wang Shaoying et al., 2009). However, the methods for imputing flux data across various flux observation networks have not been standardized. For instance, FLUXNET and the European flux network, CarboEurope, adopted the Marginal Distribution Sampling (MDS) from the mean value imputation methods and successfully applied it to the FLUXNET2015 dataset (Papale et al., 2006; Soloway et al., 2017). Meanwhile, ChinaFLUX and the Japanese flux network opted for non-linear regression methods to impute the net ecosystem exchange, while the sensible and latent heat fluxes were imputed using the day-night average transition method and the lookup table method (Li Chun et al., 2008). The Australian National Ecosystem Research Network, OzFlux, employed artificial neural network algorithms for imputation (Beringer et al., 2017), while the U.S. flux network, AmeriFlux,

https://doi.org/10.5194/egusphere-2023-2685
Preprint. Discussion started: 8 January 2024

selected both MDS and artificial neural networks to impute missing flux data (Agarwal et al., 2014). The aforementioned studies suggest that machine learning algorithms have gradually been incorporated into the domain of missing flux data imputation and have demonstrated promising performance (Moffat et al., 2007; Dengel et al., 2013; Knox et al., 2015; Beringer et al., 2017).

Machine learning technology, as a rapidly advancing super-computing domain (Ortega et al., 2023), has already demonstrated its potential value in data imputation across sectors such as transportation, healthcare, and sensor networks (Duan et al., 2014; Matusowsky et al., 2020; Gad et al., 2021). Compared to traditional machine learning techniques, the superiority of deep learning in heat flux data imputation lies not only in its capacity to integrate more environmental driving variables that affect flux exchanges but also in its prowess in handling non-linear data patterns. This is attributed to deep learning's ability to learn complex data features through multi-layer neural networks, thereby more precisely capturing intricate relationships inherent in the data. Over the past decade, deep learning has expanded from image and text processing domains to time series analysis. Specifically, Recurrent Neural Networks (RNN) and their variants, such as Long Short-Term Memory networks (LSTM) and Gated Recurrent Units (GRU), have been proven to excel in handling sequential data. They capture long-term dependencies and non-linear patterns in the data, optimizing the accuracy of time series predictions. Furthermore, the Transformer architecture, with its attention mechanism, has offered a novel approach to processing time series data, showcasing superiority in time series simulations. Convolutional Neural Networks (CNN), initially designed primarily for image recognition, have in recent years been successfully applied to the analysis and forecasting of time series data. Unlike traditional image processing, time series CNN models typically operate on one-dimensional data. CNNs capture local patterns and trends in time series data through local receptive fields and weight sharing. Local features and dependencies in time series, such as periodic patterns or breakpoints, can be efficiently captured by convolutional layers. These attributes allow CNNs to outperform traditional methods and other deep learning models in certain time series tasks, such as anomaly detection, pattern recognition, and forecasting. Concurrently, the multi-layered convolutional structure enables the model to automatically extract multi-scale features from the data. However, the practical application of deep learning in turbulent heat flux imputation remains nascent, especially in the Qinghai-Tibet Plateau region, with related studies still being sparse.

Differing from most previous research, this study aims to evaluate the capability of various artificial intelligence models in imputing the turbulent heat flux data for the QOMS site during the third Tibetan Plateau Experiment in 2012. The objective is to quantitatively compare the outcomes of different artificial intelligence models and to propose a novel turbulent heat flux imputation method based on deep learning. The ultimate goal is to complete the imputation of turbulent heat flux for this site spanning from 2007 to 2016 and make this dataset publicly accessible. The structure of this paper is organized as follows: Section 2 provides a description of the study site, instrumentation, and data processing methods; Section 3 delineates the experimental design and various data imputation methodologies; Experimental results from the application of different imputation methods are discussed in Sect. 4, while the availability of the dataset is introduced in Sect. 5; Conclusions are drawn in Sect. 6.

https://doi.org/10.5194/egusphere-2023-2685
Preprint. Discussion started: 8 January 2024

2 Materials and Methods

2.1 Site

The data used in this study originates from the third Qinghai-Tibet Plateau experiment at the QOMS station located in the bottom of the Rongbuk Valley, to the north of Mount Everest (28.36°N, 86.95°E, at an altitude of 4298m), as shown in Fig.1(adapted from Ma et al.,2020). The surface at the observation point is barren with relatively flat and open terrain, sparse and low vegetation. From the surface to the deeper soil layers, it mainly consists of sand and gravel. Not only is this observation station influenced by climate variations and weather processes, but it is also affected by local circulations of the Himalayan range, such as valley winds, making it an ideal location for monitoring surface processes on the Qinghai-Tibet Plateau.

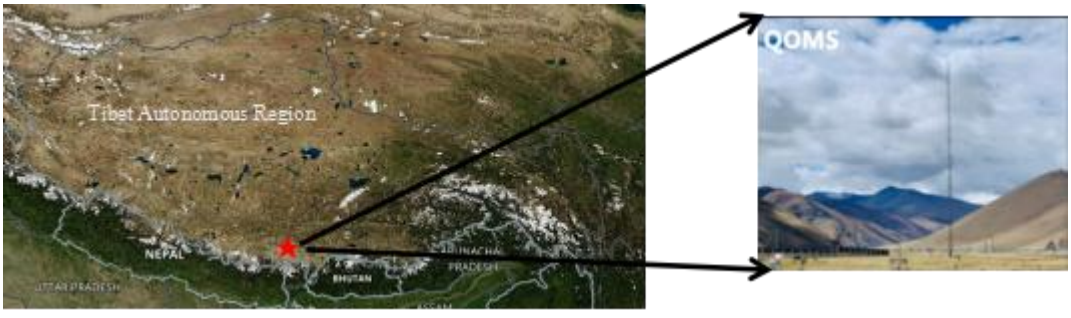

Figure 1：Geographical location and site images of the QOMS station(The map on the left is from © Google Maps, and the site on the right is adapted from Ma et al.,2020).

Figure 2 showcases the daily average time series of the main meteorological elements recorded at this observation station, reflecting the unique meteorological characteristics of the alpine region. During the observation period, the average values for temperature, relative humidity, and annual precipitation were 4.16ºC, 43.47%, and 289 mm respectively. Windspeeds observed in the winter are generally higher, reaching up to 16 m/s, while being relatively lower in the summer. During midday in the summer, surface temperatures can rise to 60 ºC, displaying a gradually increasing pattern throughout the year. Correspondingly, consistent with the annual summer rainfall pattern, surface humidity peaks in the summer.

https://doi.org/10.5194/egusphere-2023-2685
Preprint. Discussion started: 8 January 2024

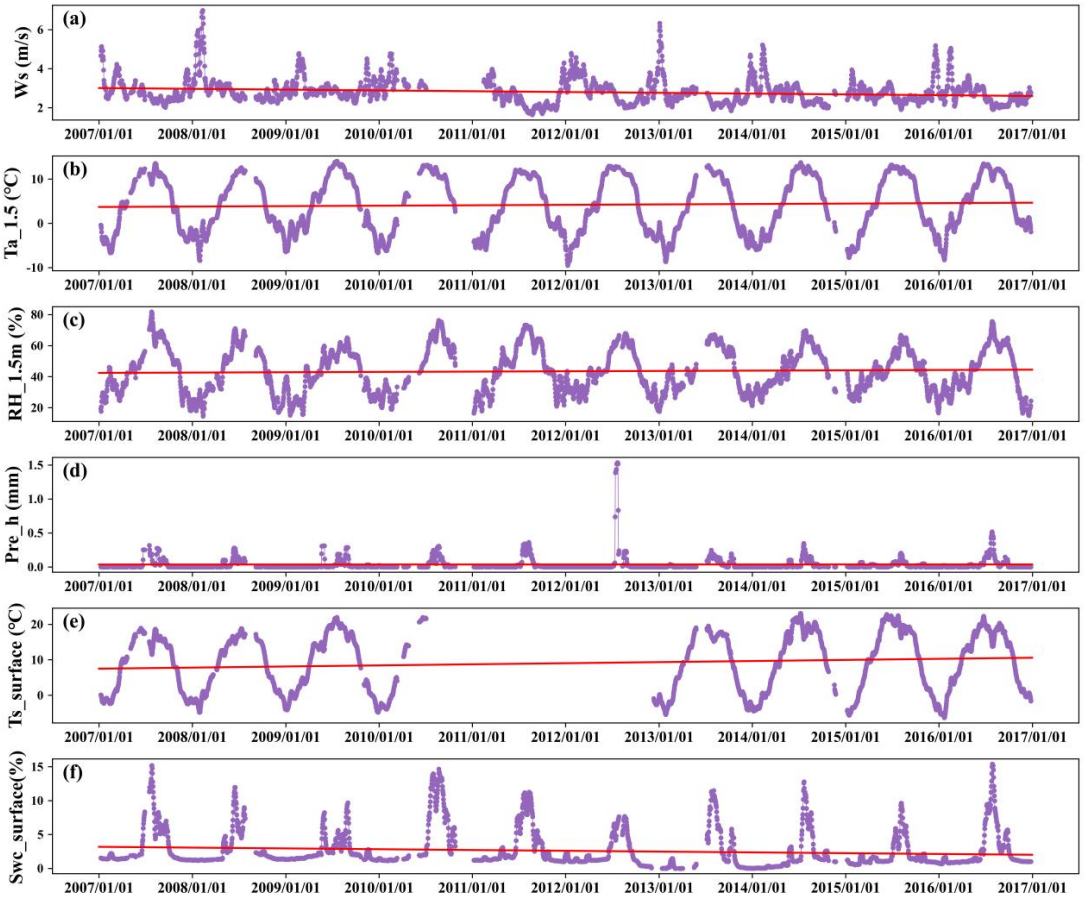

~~**Figure 2:Time series of meteorological elements collected from January 1, 2007, to December 31, 2016:(a) Wind Speed (WS);(b)Air Temperature at 1.5m height (Ta_1.5m);(c)Relative Humidity at 1.5m (RH_1.5m);(d) Hourly Average Precipitation (Prec._h);(e)Surface**~~ **Figure 2 Time series of meteorological elements collected from January 1, 2007, to December 31, 2016:(a) Wind Speed (WS);(b)Air Temperature at 1.5m height (Ta_1.5m);(c)Relative Humidity at 1.5m (RH_1.5m);(d) Hourly Average Precipitation (Prec._h);(e)Surface Temperature (Ts_surface);(f) Surface Moisture (Swc_surface).**

In recent years, many studies have focused on the climatic change characteristics of the Qinghai-Tibet Plateau, especially the phenomena of increasing temperatures and decreasing wind speeds (Yang et al., 2014). As shown in Fig. 2, a linear fit of the basic meteorological variables indicates that the temperature and relative humidity at 1.5 m and surface temperature displayed an upward trend from 2007 to 2016, while the wind speed at 1.5 m exhibited a downward trend, consistent with previous findings (Yang et al., 2014).

The Mann-Kendall (MK) trend test, with a p-value set at 0.05, offers a reliable method for identifying and quantifying potential trends in time series data. This method has been widely employed in studies in the fields of hydrology, climate change, and environmental science and has proven to be an effective tool for assessing long-term trends (Hirsch et al., 1982; Yue et al., 2002). In this study, we employed the MK trend test with a p-value set at 0.05, which likewise corroborated the

https://doi.org/10.5194/egusphere-2023-2685
Preprint. Discussion started: 8 January 2024

aforementioned results. The outcomes of the MK trend test and the fitting equations are presented in Table 1, where the unit for X in the fitting equation is hours.

Table 1:MK Statistics and Fitting Equations

Indicator	MK Statistic	P-value	Fitting Equation	Trend
WS_1.5m	-0.036	$4.48e^{-51}$	$Y = -5.19\times10^{-8}X + 3.01$	Downward
Ta_1.5	0.023	$3.90e^{-23}$	$Y = 1.19\times10^{-5}X + 3.69$	Upward
RH_1.5	0.017	$7.19e^{-13}$	$Y = 2.26\times10^{-5}X + 42.43$	Upward
Prec_h	0.023	$4.60e^{-16}$	$Y = 1.75\times10^{-8}X + 0.03$	Upward
Ts_surface	0.017	3.14^{-10}	$Y = 4.99\times10^{-5}X + 7.49$	Upward
Swc_surface	-0.19	0	$Y=-1.44\times10^{-5}X+3.18$	Downward

2.2 Site Data

This study analyzes the observational data from the QOMS observation site from January 1, 2007, to December 31, 2016. Specific variables include: sensible heat flux H, latent heat flux LE, soil heat flux SHF, air temperature at five levels Tair (1.5, 2, 4, 10, 20 m), relative humidity at five levels RH (1.5, 2, 4, 10, 20 m), wind speed at five levels WS (1.5, 2, 4, 10, 20 cm), wind direction at five levels WD(1.5, 2, 4, 10, 20 cm), downward shortwave radiation Rsd, upward shortwave radiation Rsu, downward longwave radiation Rld, upward longwave radiation Rlu, soil temperature at six levels Tsoil(0, 0.1, 0.2, 0.4, 0.8, 1.6 m), and soil volumetric water content at six levels SWC(0, 0.1, 0.2, 0.4, 0.8, 1.6 m). The instruments used at the site are shown in Table 2.

Table 2:Installation Heights and Burial Depths of the Observation Instruments

Variables	Sensor models	Manufacturers	Heights	Units
Air temperature	HMP45C-GM	Vaisala	1.5,2,4,10and20m	ºC
Wind speed and direction	034B	MetOne	1.5,2,4,10and20m	ms^{-1}/º
Humidity	HMP45C-GM	Vaisala	1.5,2,4,10and20m	%
Pressure	PTB220A	Vaisala	-	hPa
Radiations	CNR1	Kipp&Zonen	-	Wm^{-2}
Precipitation	RG13H	Vaisala	-	mm
Soil temperature	Model107	Campbell	0,0.1,0.2,0.4,0.8and1.6m	◦C
Soil moisture	CS616	Campbell	0,0.1,0.2,0.4,0.8and1.6m	v/v%

https://doi.org/10.5194/egusphere-2023-2685
Preprint. Discussion started: 8 January 2024

Soil heat flux	HFP01	Hukseflflux	0.05m	Wm^{-2}
H	CSAT3	Campbell	3.25m	Wm^{-2}
LE	LI-7500	Li-COR		

From 2007 to 2016, the missing rates for H and LE at the observation site (including missing and distorted data), denoted as gap_H and gap_LE, were 21.7 % and 21.4 % respectively (Table 3).

Table 3:Missing Rates for Sensible Heat Flux and Latent Heat Flux

	2007	2008	2009	2010	2011	2012	2013	2014	2015	2016
gap_H	39.4%	10.3%	22.2%	9.8%	32.2%	29.6%	11.7%	10.4%	18.1%	33.3%
gap_LE	37.65%	8.28%	21.30%	8.48%	23.63%	28.52%	9.90%	8.84%	33.57%	33.34%

2.3 Data Preprocessing

To interpolate missing flux data using machine learning algorithms, it is essential to ensure the completeness of environmental driving variables (Wang Shaoying et al., 2009). Therefore, during the data preprocessing phase, this study employed the K-Nearest Neighbors (K-NN) interpolation method to address the missing data of environmental driving variables. The number of neighbors was set to 3, and "distance" was used as the weight calculation method to ensure that observations closer in distance have higher weights (Friedman et al., 2009). The equation is given by Eq. (1).

$$\text{Gap\_filling value} = \frac{\sum_{i=1}^{3} \frac{y_i}{d_i}}{\sum_{i=1}^{3} \frac{1}{d_i}} \quad (1)$$

Where:

y_i is the observation of the ith nearest neighbor;

d_i is the distance between the missing value and the ith nearest neighbor;

The numerator involves the weighted sum based on the observations and the reciprocal of the distances of the 3 nearest neighbors;

The denominator is the sum of the reciprocals of the distances for these 3 nearest neighbors.

Subsequently, the "fit_transform" method is utilized to fit and transform the chosen data, facilitating the imputation of missing values. Lastly, the imputed data is merged with the original sensible and latent heat fluxes to derive a comprehensive dataset of environmental driving variables.

This K-NN-based imputation method proves effective when handling data with similar patterns or local consistency (Little and Rubin, 2002). By considering the distances between observation points over time, this approach can accurately estimate missing values, ensuring greater reliability of the data in subsequent analyses.

https://doi.org/10.5194/egusphere-2023-2685
Preprint. Discussion started: 8 January 2024

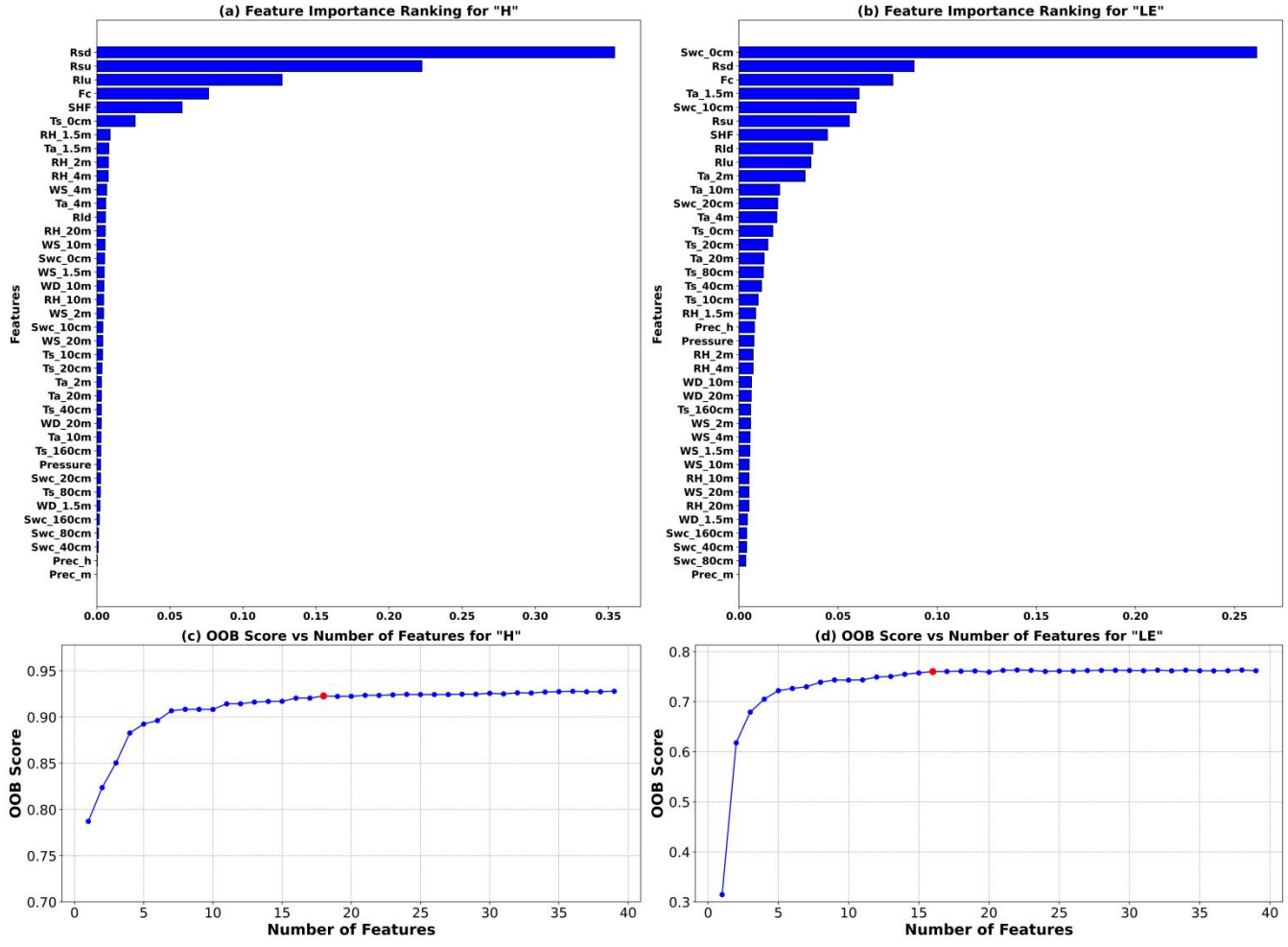

Figure 3:(a) Importance index for sensible heat flux (H), (b) Importance index for latent heat flux (LE), (c) OOB scores for different feature combinations of sensible heat flux based on Random Forest (the red dot indicates the maximum value), (d) OOB scores for different feature combinations of latent heat flux based on Random Forest (the red dot indicates the maximum value).

By ranking the features according to their importance, the Random Forest selects the optimal feature combination, effectively reducing the dimensionality of the input features and guiding the selection of variables in machine learning models. In this study, based on ten-fold cross-validation and grid search algorithms, the number of estimators in the Random Forest model was set to 159, meaning the model consists of 159 decision trees. As bootstrapping (sampling with replacement) was employed to generate random decision trees, not all samples participate in the tree generation process. The unused samples are termed out-of-bag (OOB) samples. Through these OOB samples, the accuracy of the tree can be assessed.

Before training the model, it is necessary to determine whether all 39 trajectory features influence the prediction results. Figure 3a displays the importance order of the remaining 39 features for the sensible heat flux calculated using the Random

https://doi.org/10.5194/egusphere-2023-2685
Preprint. Discussion started: 8 January 2024

Forest method; Figure 3b presents the importance order of the remaining 39 features for the latent heat flux. The results indicate that for subsequent turbulence heat flux fitting, characteristics such as radiation, air temperature, soil temperature, and soil humidity have a higher importance. However, whether to exclude some less important features requires further consideration.

The OOB scores under different input feature dimensions have been calculated, with variables input in order of importance, as shown in Fig. 3c. For the sensible heat flux, the OOB score is highest when considering the top 18 features ranked by importance; as shown in Fig. 3d, for the latent heat flux, the OOB score peaks when considering the top 16 features. Additional features added afterward no longer impact the results; in other words, the optimal combination for sensible heat comprises the top 18 features, and for latent heat, it's the top 16 features.

3 Experiments

3.1 Experimental design

The aim of this study is to use a decade's worth of observational data to fit missing values for sensible and latent heat fluxes. We explored the turbulence flux changes at the QOMS site from 2007 to 2016 and treated the missing parts of the turbulence flux in the dataset as quantitative prediction variables. The objective is to impute these missing data, forming a complete heat flux dataset.

In the research application of the model, it is crucial to correctly divide the training, validation, and test sets (Bishop and M, 2006; Friedman et al., 2009). The training set is used to train the model's parameters so that the model can learn and capture the underlying patterns and structures from the given data (Goodfellow et al., 2016). The primary purpose of the validation set is for model selection and hyperparameter tuning, enhancing the model's generalization capability (Cawley and Talbot, 2010). The test set offers a completely independent evaluation method to more accurately assess the model's performance on unseen data (Arlot and Celisse, 2010). This dataset has never been used in the training or validation process, so it can serve as an unbiased estimate of the model's performance in practical applications (Kohavi, 1995). Due to the severe missing turbulence heat flux data in 2012, based on the interpolation dataset length and research objective, all samples are divided into the following three groups: training set (2007-2011, 2013-2016); 10% of the samples randomly extracted from the training set as the validation set; test set (2012). In total, there are 87,673 samples, of which 80% are used for training, 10% for validation, and the remaining 10% for testing.

This design plan fully considers the complexity and diversity of time series analysis while ensuring the rigor of model validation and testing. In this way, it provides an accurate and reliable means to predict soil turbulence heat flux.

3.2 Traditional machine learning methods

In the traditional machine learning domain, various algorithms have been widely applied for data fitting and prediction. The Support Vector Machine (SVM) is a linear classifier, with the goal of finding an optimal hyperplane that maximizes the

https://doi.org/10.5194/egusphere-2023-2685
Preprint. Discussion started: 8 January 2024

margin between two different classes of data points, ensuring optimal classification performance (Cortes and Vapnik, 1995). XGBoost is an optimized gradient boosting algorithm that enhances the model's performance by progressively adding new trees and adjusting the errors of previous trees. It has been proven to perform excellently in various competitions and practical applications (Chen et al., 2016). The K-Nearest Neighbors (KNN) algorithm is an instance-based learning method. It classifies or predicts by calculating the distance between the input data point and the data points in the training dataset, selecting the nearest K points, and voting based on their labels (Cover and Hart, 1967). Each algorithm has its unique principle, offering multiple choices for addressing the problem of turbulent heat flux imputation.

3.3 Recurrent neural network

Recurrent Neural Networks (RNNs) are a class of deep learning models designed for processing sequential data. The core idea is to share weights between the hidden layers of the network to capture temporal dependencies within sequences. However, standard RNNs suffer from issues of vanishing and exploding gradients, which limit their ability to capture long-term dependencies. Long Short-Term Memory networks (LSTM) address this problem by introducing special units with three gate structures, allowing the network to learn and remember long-term dependencies within sequences. Gated Recurrent Units (GRUs) are a variant of LSTM that improve computational efficiency by simplifying the gate structure and reducing the number of parameters, while retaining the ability to capture long-term dependencies. These recurrent neural network architectures have achieved significant success in many sequence modeling and prediction tasks.

3.4 Transformer

The Transformer model is a deep learning architecture widely used in natural language processing and other sequence-to-sequence tasks (Vaswani et al., 2017). It mainly consists of two parts: an encoder and a decoder. Transformers capture long-distance dependencies in sequences through the self-attention mechanism. Self-attention allows the model to consider other positions in the input sequence simultaneously at all positions, which, unlike traditional RNNs and LSTMs, eliminates the need for sequential computation, thereby greatly enhancing parallel computation capabilities. Following each self-attention layer is a feed-forward neural network, accompanied by layer normalization, which contributes to training stability and convergence. The Transformer exhibits outstanding performance in data fitting and prediction. Its ability for parallel computation allows it to process large datasets more quickly. The self-attention mechanism ensures that the model can capture complex dependencies, surpassing previous methods in many tasks.

3.5.Transformer_CNN

To address the high complexity of data from the Qinghai-Tibet Plateau, a deep neural network model based on the PyTorch framework was adopted in this study, as illustrated in Fig. 4. At the initialization of the model, a layer normalization component was introduced with the aim of normalizing the input along the embedding dimension, thereby enhancing the stability and convergence rate of network training. Subsequently, a feed-forward neural network comprising three fully

https://doi.org/10.5194/egusphere-2023-2685
Preprint. Discussion started: 8 January 2024

connected layers was defined, incorporating a ReLU activation function to capture non-linear features. The output embedding dimension was determined by "emb_dim". Three one-dimensional convolutional layers with varying kernel sizes were then introduced with the intent of capturing local features at different temporal scales, such as the multi-periodicity of turbulent heat fluxes. Following this, another one-dimensional convolutional layer was defined to integrate the outputs from the previous three convolutional layers, forming a comprehensive feature representation.

The multi-head self-attention mechanism was realized through the Multi-Head Attention component, which boasts four attention heads capable of capturing long-distance dependencies within the input sequence. The Decoder section of the model is responsible for mapping the encoded features to the target space. To ensure the stability of the model, the Weight Initialization component ascertained a scientific initialization of weights and biases.

The forward propagation process was defined by the feed-forward function, and ultimately, when the model is invoked, two data views are generated: F1 (primary view) and F2 (contrast view). Despite the presence of dropout, the two views might still differ. The loss function employed is the Smooth L1 Loss, comprised of three parts: the loss between F1 and the true value, the loss between F2 and the true value, and the distance between F1 and F2, which serves as a regularization term multiplied by 0.1. During model inference, the final prediction is derived from the average of F1 and F2.

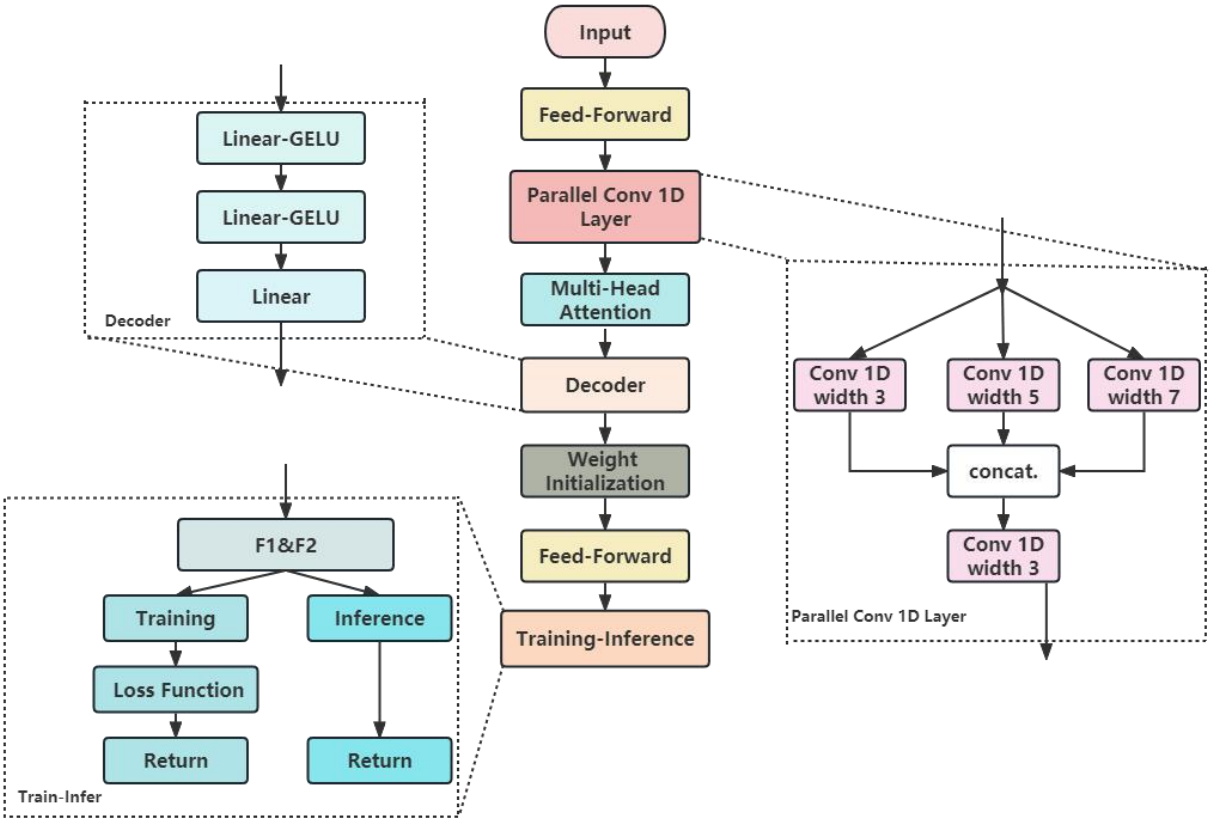

Figure 4:The model framework and network structure of Transformer_CNN.

https://doi.org/10.5194/egusphere-2023-2685
Preprint. Discussion started: 8 January 2024

4 Results

Three types of traditional machine learning methods(SVM, KNN, and XGBoost)were initially employed to train on different feature samples for sensible heat flux and latent heat flux. These features were selected by the random forest method based on their importance. Subsequently, Bayesian optimization was utilized to identify the model that best fits the data samples. Training then proceeded with two types of recurrent neural networks and the Transformer model, with the features selected in a similar manner as mentioned earlier. With the number of output channels set to 128, three convolutional layers transformed the input one-dimensional data into feature maps endowed with 128 features. This approach enhanced the richness of information within the network and allowed subsequent layers to learn from a more complex and diversified feature representation. To prevent overfitting, early stopping was employed. Training was halted once the model's performance on the validation set began to decline, averting potential overfitting that could arise from continued training.

The performance of the six models was assessed by calculating the RMSE and MAE values between the predicted and actual values for both the sensible and latent heat fluxes. These evaluations are presented in Table 1, encompassing the training, validation, and test sets, with the best results highlighted in bold. Evidently, among the three traditional machine learning methods, the SVM model demonstrated superior performance in simulating the sensible heat flux, whereas XGBoost excelled in simulating the latent heat flux. Surprisingly, both RNN models exhibited subpar performance in the task of simulating turbulent fluxes. Two predominant factors might account for these observations. One pertains to the challenges of gradient vanishing and explosion. Although LSTM and GRU structures are crafted to counteract gradient vanishing, due to the complex non-linear variations of turbulent heat fluxes, this issue can emerge during simulations. The second factor concerns the nuances of hyperparameter optimization in RNN models. Choosing the right set of hyperparameters, which are particularly numerous in RNNs, is crucial to achieving optimal model performance. Fortunately, the Transformer model showcased exceptional prowess in the task of simulating turbulent fluxes. In almost all simulations, the Transformer model achieved the best performance, boasting the smallest RMSE and MAE on the test set. As a result, the Transformer model architecture was integrated into the neural network framework, and by further incorporating convolutional layers and multi-head attention mechanisms, a Transformer_CNN model was proposed, which was found to be superior in simulating turbulent fluxes.

Table 4:Model performance evaluation (RMSE and MAE) for SVM, KNN, XGBoost, LSTM, GTU, and Transformer. Bold values highlight the best performance.

Sets	H						LE					
	Training		Validation		Test		Training		Validation		Test	
	RMSE	MAE	RMSE	MAE	RMES	MAE	RMSE	MAE	RMSE	MAE	RMES	MAE
SVM	19.38	2.856	19.88	2.965	25.89	3.182	25.12	3.093	21.12	3.174	19.79	3.124
KNN	20.83	2.946	25.18	3.016	31.41	3.519	**14.61**	**2.692**	19.99	3.095	20.05	3.271

https://doi.org/10.5194/egusphere-2023-2685
Preprint. Discussion started: 8 January 2024

XGBoost	25.58	3.124	25.07	3.549	29.34	4.178	16.21	2.977	19.11	3.066	16.88	3.034
LSTM	25.13	3.029	24.59	3.481	28.68	4.159	18.86	2.859	20.72	3.017	19.47	3.033
GRU	22.14	3.004	21.74	3.257	26.99	4.036	17.59	2.818	21.76	3.157	20.96	3.198
Transformer	**16.65**	**2.531**	**18.07**	**2.814**	**24.04**	**3.029**	18.15	2.883	**19.10**	**3.079**	**14.57**	**2.830**

Table 5 juxtaposes the results of the Transformer_CNN with various artificial intelligence models, illustrating the predictive outcomes in terms of the coefficient of determination (R^2). Evidently, the Transformer_CNN possesses a distinct advantage in long-term predictions. The performance of the Transformer_CNN model in data fitting surpassed that of the conventional Transformer model. Firstly, the incorporation of the Convolutional Neural Network (CNN) enhanced the model's capability to extract local features (Lecun et al., 1998). The CNN, through its convolutional layers, manages to capture the evident seasonal and cyclical variations in turbulent heat fluxes. By identifying these local patterns, it discerns the daily, monthly, and seasonal variations in turbulent fluxes, thereby holding an edge in capturing intricate patterns within the data (Krizhevsky et al., 2012). Secondly, predicting turbulent heat fluxes encompasses intricate physical processes and multi-scale interactions. The prowess of the Transformer model in capturing long-distance dependencies (Vaswani et al., 2017), combined with the CNN's local feature extraction capability, facilitates a superior grasp of the interactions among wind speed, temperature, and radiation with respect to turbulent heat fluxes, thereby enhancing the model's versatility and diversity. Moreover, the efficiency of convolutional operations might contribute to elevating the speed and efficiency of model training (Goodfellow et al., 2016). By employing a hybrid model of CNN and Transformer, both local and global features can be concurrently captured, thereby manifesting an adaptive advantage in data fitting for turbulent heat fluxes (Bello et al., 2019). In summary, the Transformer_CNN model, by amalgamating the Transformer's global dependency capture capability with the CNN's local feature extraction prowess, offers a richer and more flexible model representation, thereby exhibiting superior performance in data fitting

.

Table 5:Comparison of the Coefficient of determination(R^2) predicted by multiple models. Bold values highlight the best performance.

	H			LE		
Sets	Training	Validation	Test	Training	Validation	Test
SVM	0.92	0.91	0.90	0.78	0.80	0.82
KNN	0.91	0.90	0.85	0.86	0.78	0.79
XGBoost	0.90	0.90	0.87	0.83	0.78	0.85
LSTM	0.93	0.93	0.88	0.82	0.80	0.83
GRU	0.94	0.94	0.89	0.84	0.78	0.81
Transformer	0.93	0.93	0.91	0.85	0.81	0.87

https://doi.org/10.5194/egusphere-2023-2685
Preprint. Discussion started: 8 January 2024

Transformer_CNN	**0.94**	**0.94**	**0.95**	**0.90**	**0.81**	**0.90**

To comprehensively assess the reliability and efficacy of the Transformer_CNN model in estimating turbulent heat fluxes (H and LE), this study employed a Taylor diagram for comparative analysis with six other advanced artificial intelligence models. The Taylor diagram serves as an effective tool for quantifying the correlation and discrepancies between model predictions and observed data. Within the diagram, angles represent the correlation coefficient between model predictions and observed values; the bold dashed line signifies the standard deviation of model predictions, while the light-colored semi-circle dashed line represents the root mean square error (RMSE) between the model predictions and the actual values. As a reference benchmark, the EC (eddy covariance) observed values were used to evaluate the performance of each model. The results, as depicted in Fig. 5, detail the performance of each model on the test set. Encouragingly, the Transformer_CNN model's estimation of turbulent heat fluxes, whether viewed from the RMSE or correlation coefficient perspective, markedly surpasses the other six artificial intelligence models. Specifically, the Transformer_CNN model exhibits the smallest RMSE, with 0.29 for sensible heat flux and 0.31 for latent heat flux, while its model correlation coefficient consistently exceeds 0.94, again outperforming the other six AI models. These outcomes not only validate the model's exemplary performance in fitting turbulent heat fluxes but also underscore its superior generalization capability. Compared to traditional statistical methods and other artificial intelligence techniques, the Transformer_CNN model offers a more precise and robust solution, bearing significant practical implications for areas like climate research and meteorological forecasting.

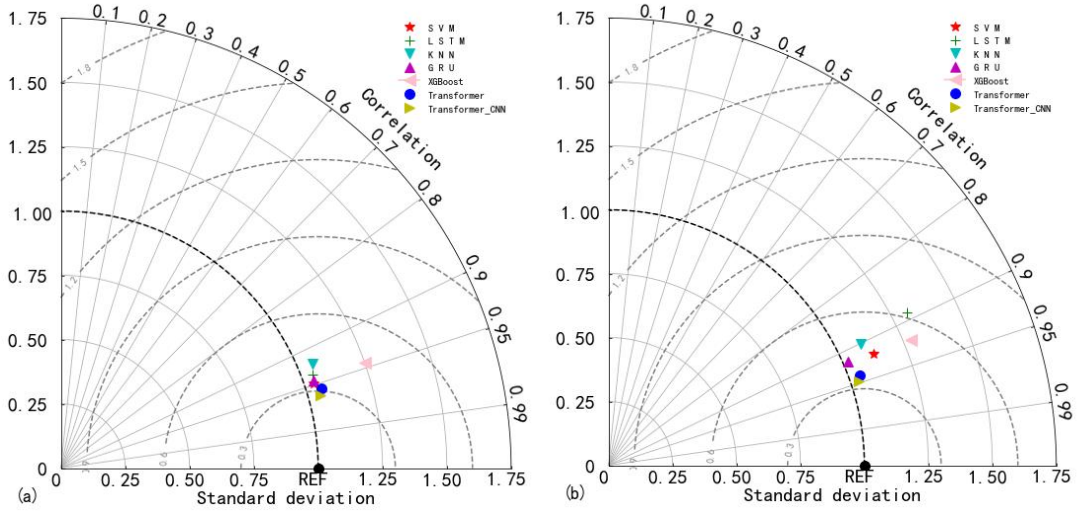

Figure 5:The Taylor diagram displays the performance of seven models on the test set data: a) Sensible heat flux (H); b) Latent heat flux (LE).

https://doi.org/10.5194/egusphere-2023-2685
Preprint. Discussion started: 8 January 2024

To more comprehensively and intuitively describe the Transformer_CNN, Fig. 6 displays a scatter plot of predicted values against actual values. The distance between the data points and the diagonal line indicates prediction errors. The results suggest that the majority of the turbulent heat flux values are centered around 0. Owing to the large volume of low-value data, the model is adept at capturing the characteristics of environmental driving forces when observed values are near 0, thereby achieving more accurate predictions. As observed values increase, the prediction error of the model gradually amplifies. Furthermore, it was observed that when the turbulent heat flux is substantial, predicted values typically fall below the observed values. This phenomenon is more pronounced in the fitting of LE.

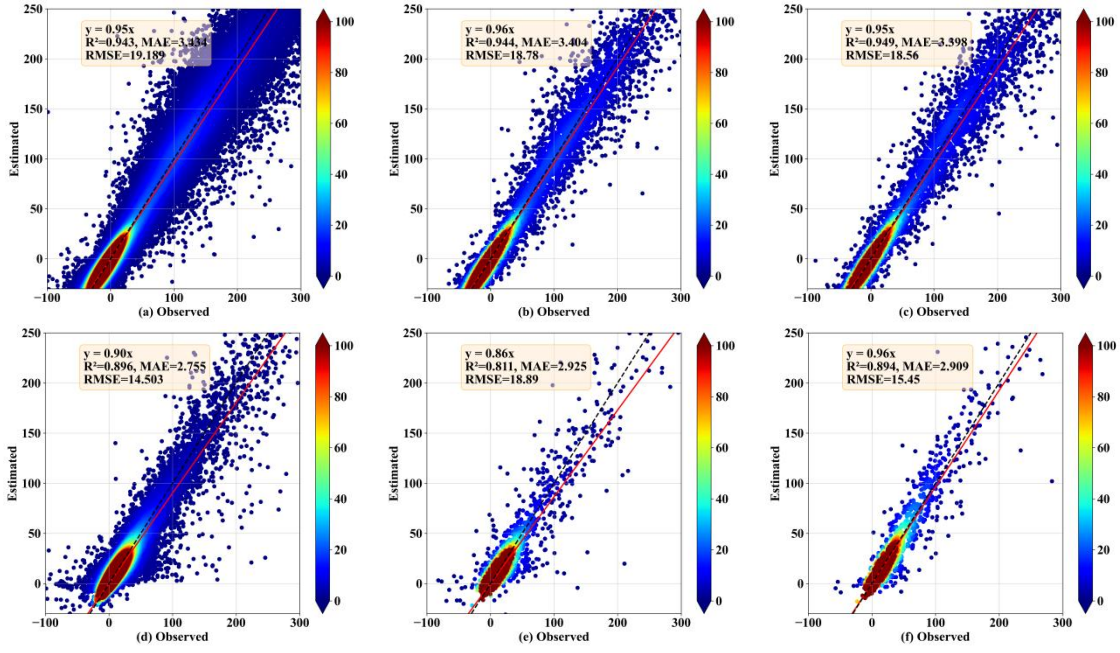

Figure 6:Scatter density plots of observed values and Transformer_CNN estimated values, where a) and d) are for the training dataset, b) and e) are for the validation dataset, and c) and f) are for the test dataset. a), b), and c) are estimates for H, while d), e), and f) are estimates for LE.

To better display the predictions of the Transformer_CNN model, Fig. 7a and Fig. 7b respectively show the monthly average diurnal variation curves for H and LE in the test set. The red line represents observed values, while the blue and green lines represent the predictions of the Transformer and Transformer_CNN models respectively.

In the prediction of sensible heat flux, both the Transformer and Transformer_CNN models perform excellently for the hours of 0-9 and 19-23, where their predicted values closely align with the observed values. However, between 9-19 hours, as solar radiation intensity increases and the sensible heat flux rapidly grows, the Transformer model struggles to capture this escalating trend, resulting in a notable underestimation. The Transformer_CNN model, having incorporated convolutional layers, is better equipped to recognize periodic data changes and the impacts of environmental drivers on sensible heat, substantially rectifying the underestimation issues observed in high values.

https://doi.org/10.5194/egusphere-2023-2685
Preprint. Discussion started: 8 January 2024

In the latent heat flux prediction, the performance superiority of the Transformer_CNN model is even more pronounced. While the Transformer model exhibits significant over estimations in low-value periods and struggles to capture high values, the Transformer_CNN model's predictions largely coincide with observed values, significantly reducing the prediction errors exhibited by the Transformer model. Not only does it excel during the low-value periods of LE in January-March and October-December, but it also accurately predicts the pronounced increase of LE in July-September. The experiments demonstrate that the Transformer_CNN model is well-suited to serve as an artificial intelligence model for imputing turbulent heat fluxes.

https://doi.org/10.5194/egusphere-2023-2685
Preprint. Discussion started: 8 January 2024

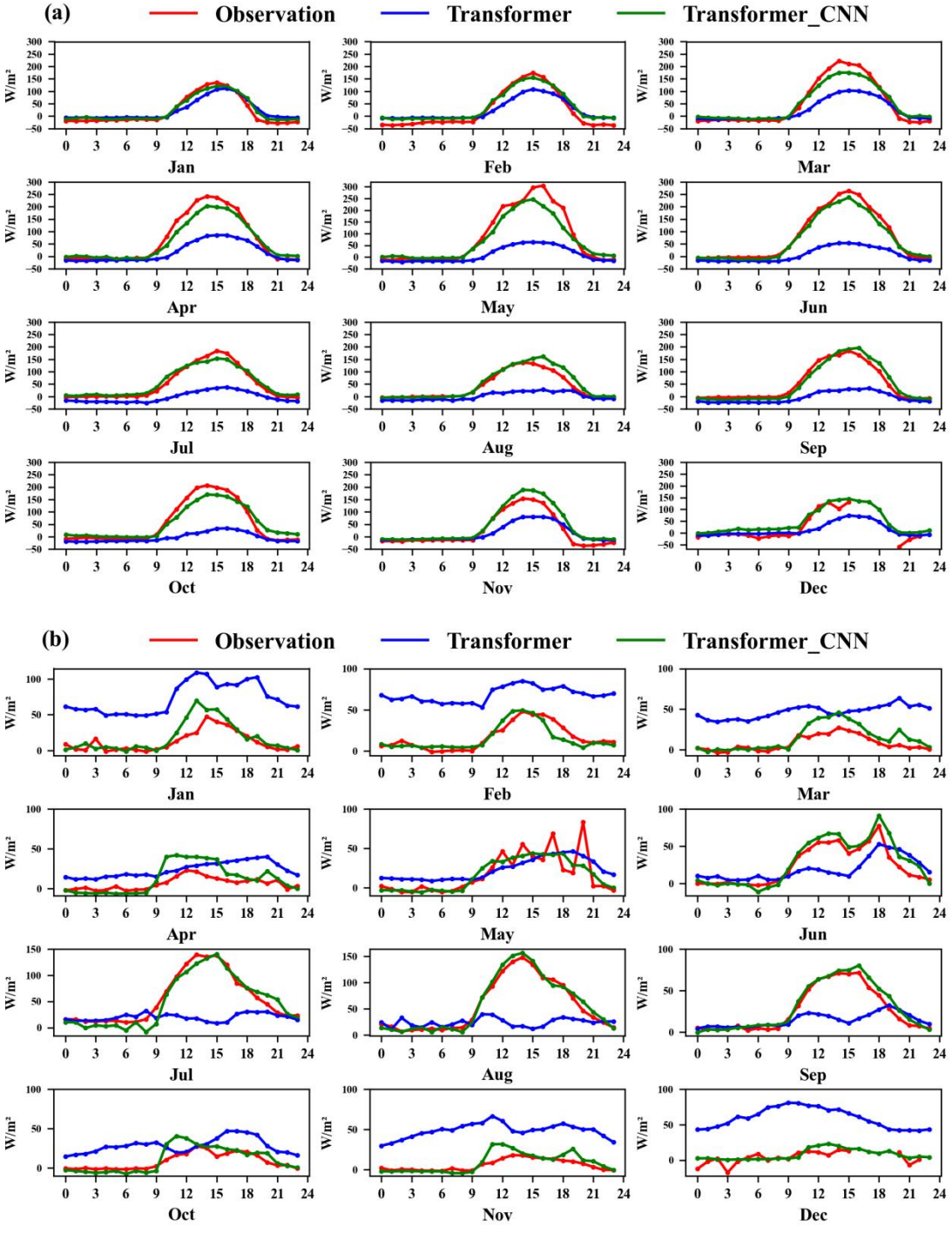

365

https://doi.org/10.5194/egusphere-2023-2685
Preprint. Discussion started: 8 January 2024

Figure 7:Observed values, Transformer estimated values, and Transformer_CNN estimated values for the monthly average diurnal variation curves in the test set (2012) are shown. Specifically, (a) represents the sensible heat flux (H), and (b) represents the latent heat flux (LE).

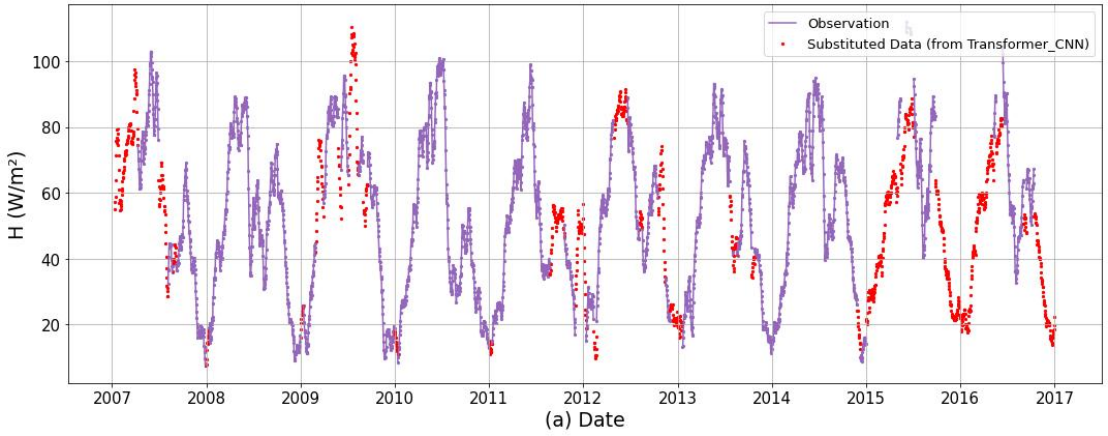

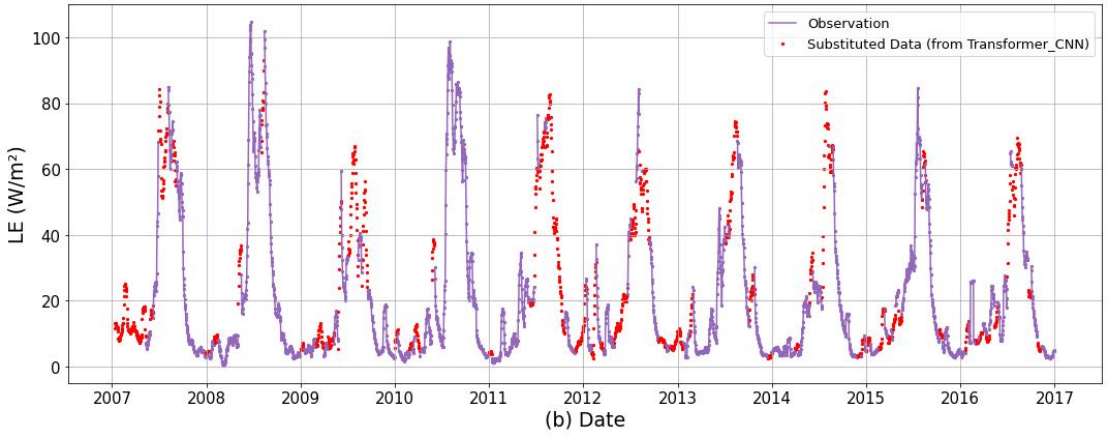

Figure 8:Observed values and Transformer_CNN estimated values for the variation curves from 2007 to 2016 are presented. Specifically, (a) depicts the sensible heat flux (H), and (b) illustrates the latent heat flux (LE).

Based on the research presented earlier, it was determined that the Transformer_CNN model can serve as an artificial intelligence model for imputing turbulent heat fluxes. To delve deeper into the variation of turbulent heat fluxes at the QOMS site, the model was employed to impute data from 2007 to 2016 for the QOMS site, with the results shown in Figure 8. The variation in sensible heat flux, as depicted in Figure 8a, indicates that prior to the monsoon season, the sensible heat flux is the primary consumer of the available energy at the Earth's surface. With the onset of the summer monsoon, the diurnal variation of sensible heat flux significantly decreases, equating to the latent heat flux. In other words, during the pre-monsoon period, the exchange of sensible heat flux dominates. Influenced by the interaction of mid-latitude westerlies and the summer monsoon, the summer sensible heat flux is significantly lower than that of the spring. In contrast to the bi-modal

https://doi.org/10.5194/egusphere-2023-2685
Preprint. Discussion started: 8 January 2024

seasonal variation of sensible heat flux, the seasonal variation of latent heat flux exhibits a single peak pattern. That is, during the pre-monsoon period, the latent heat flux is small, but with the outbreak of the monsoon, it rapidly increases due to frequent precipitation and the moistening of the surface soil. Subsequently, the latent heat flux gradually increases, equating to the sensible heat flux during the summer monsoon period. A comparison of the seasonal variations of the sensible heat flux (Fig. 8a) and the latent heat flux (Fig. 8b) suggests that during the Asian summer monsoon season, the impacts of latent and sensible heat fluxes at the QOMS site are comparable; during the non-monsoon season in Asia, the site's sensible heat flux has a greater impact.

5 Conclusions

During the period from 2007 to 2016, deep learning methods were employed to impute turbulent heat flux observational data for the QOMS site. To optimize predictive performance and simplify model complexity, we first utilized the random forest algorithm to extract features from basic meteorological, turbulent, radiation, and soil data, eliminating redundant data. Subsequently, three traditional machine learning methods (SVM, XGBoost, KNN) were adopted, along with two recursive neural networks (LSTM, GRU) and the deep learning model, Transformer, introduced in 2017, for model evaluation and comparison. The results indicated that the Transformer exhibited superior performance in imputing turbulent heat fluxes.

To further optimize predictive performance, CNN was introduced and combined with the Transformer, forming a new model named Transformer_CNN. The CNN was designed to capture the periodic change features of turbulent heat fluxes across different time scales, while the Transformer effectively captured long-distance dependencies in time-series data, aiding in revealing intricate temperature variation patterns under environmental driving variables more precisely. Upon evaluation, Transformer_CNN significantly outperformed other traditional artificial intelligence models in terms of predictive performance.

More specifically, Transformer_CNN excelled in predicting H, with a determination coefficient (R^2) for its test set reaching 0.949. It could predict not only low values accurately but also achieved precise predictions as observed values increased, addressing the shortcomings of the traditional Transformer model in predicting higher values. In terms of predicting LE, its test set determination coefficient reached 0.894, effectively resolving the issues of overestimation of low values and underestimation of high values by the Transformer model. In summary, the experimental results thoroughly validated that the Transformer_CNN model provides a novel and efficient solution for imputing turbulent heat fluxes.

Lastly, the Transformer_CNN model was utilized to impute turbulent heat flux data from 2007 to 2016 for the QOMS site. It was found that during non-monsoon periods, H dominated. However, during the summer monsoon season, influenced by the interactions of mid-latitude westerlies and the monsoon, the H decreased and became similar to the latent heat flux. Overall, during the summer, the impacts of H and LE fluxes at the QOMS site were comparable, while the influence of H was more pronounced during non-monsoon periods.

https://doi.org/10.5194/egusphere-2023-2685
Preprint. Discussion started: 8 January 2024

Author contributions

GZ and HQ designed the experiments and carried them out. GZ, HQ and DZ performed data processing, organization, and figure generation. GZ, HQ and DZ wrote the manuscript, and all authors participated in the revision of the paper.

Competing interests

The contact author has declared that none of the authors has any competing interests.

Code and data availability

The dataset and code are both available at https://doi.org/10.5281/zenodo.10005741 (Hou et al., 2023). The local time (UTC+8) was used at the site.

Acknowledgements

We sincerely thank all the scientists, engineers, and students who participated in the field surveys, maintained the measurement instruments, and processed the observational data. We are deeply grateful to the anonymous reviewers for their valuable comments and suggestions.

Financial support

This work was funded by the Second Tibetan Plateau Scientifc Expedition and Research Program (Grant 2019QZKK0102).

References

Agarwal, D., Pastorello, G., Poindexter, C., Papale, D., Trotta, C., Ribeca, A., Canfora, E., Faybishenko, B., and Samak, T.: The data post-processing pipeline for AmeriFlux data products, Agu Fall Meeting, ui.adsabs.harvard.edu/abs/2014AGUFM.B53A0159A, 2014.

Arlot, S. and Celisse, A.: A survey of cross-validation procedures for model selection, Statistics Surveys, 4, 40-79, 10.1214/09-SS054, 2010.

Baldocchi, D.: Measuring fluxes of trace gases and energy between ecosystems and the atmosphere - the state and future of the eddy covariance method, Glob. Change Biol., 20, 3600-3609, 10.1111/gcb.12649, 2014.

Baotian, P., Jijun, L., and Fahu, C.: Qinghai-Tibetan Plateau: a Driver and Amplifier of Global Climatic Changes——I Basic Characteristics of Climatic Changes in Cenozoic Era, Journal of Lanzhou University(Natural Sciences), 32, 108-115, 10.13885/j.issn.0455-2059.1995.03.024, 1996.

https://doi.org/10.5194/egusphere-2023-2685
Preprint. Discussion started: 8 January 2024

Bello, I., Zoph, B., Vaswani, A., Shlens, J., Le, Q. V., and Ieee: Attention Augmented Convolutional Networks, IEEE/CVF International Conference on Computer Vision (ICCV), Seoul, SOUTH KOREA, Oct 27-Nov 02, WOS:000531438103044, 3285-3294, 10.1109/iccv.2019.00338, 2019.

Beringer, J., McHugh, I., Hutley, L. B., Isaac, P., and Kljun, N.: Technical note: Dynamic INtegrated Gap-filling and partitioning for OzFlux (DINGO), Biogeosciences, 14, 1457-1460, 10.5194/bg-14-1457-2017, 2017.

Bishop and M, C.: Pattern Recognition and Machine Learning, Springer-Verlag, New York, 10.1007/978-3-030-57077-4_11, 2006.

Cawley, G. C. and Talbot, N. L. C.: On Over-fitting in Model Selection and Subsequent Selection Bias in Performance Evaluation, J. Mach. Learn. Res., 11, 2079-2107, 10.5555/1756006.1859921, 2010.

Chapin, F. S., Matson, P. A., and Mooney, H. A.: Principles of Terrestrial Ecosystem Ecology, Springer Verlag, Seconded, New York, USA, 10.1007/978-1-4419-9504-9, 2011.

Chen, B., Chao, W. C., Liu, X. J. C. d. O., theoretical, and system, c. r. o. t. c.: Enhanced climatic warming in the Tibetan Plateau due to doubling CO2: a model study, 20, 10.1007/s00382-003-0308-6, 2003.

Chen, T. Q., Guestrin, C., and Assoc Comp, M.: XGBoost: A Scalable Tree Boosting System, 22nd ACM SIGKDD International Conference on Knowledge Discovery and Data Mining (KDD), San Francisco, CA, Aug 13-17, WOS:000485529800092, 785-794, 10.1145/2939672.2939785, 2016.

Collatz, G. J., Bounoua, L., Los, S. O., Randall, D. A., Fung, I. Y., and Sellers, P. J.: A mechanism for the influence of vegetation on the response of the diurnal temperature range to changing climate, 27, 3381-3384, 10.1029/1999GL010947, 2000.

Cortes, C. and Vapnik, V.: Support-vector networks, Machine Learning, 20, 273-297, 10.1007/BF00994018, 1995.

Cover, T. and Hart, P.: Nearest neighbor pattern classification, IEEE Transactions on Information Theory, 13, 21-27, 10.1109/TIT.1967.1053964, 1967.

Defries, R. S., Bounoua, L., and Collatz, G. J.: Human modification of the landscape and surface climate in the next fifty years, 8, 438-458, 10.1046/j.1365-2486.2002.00483.x, 2002.

Dengel, S., Zona, D., Sachs, T., Aurela, M., Jammet, M., Parmentier, F. J. W., Oechel, W., and Vesala, T.: Testing the applicability of neural networks as a gap-filling method using CH4 flux data from high latitude wetlands, Biogeosciences, 10, 8185-8200, 10.5194/bg-10-8185-2013, 2013.

Duan, Y. J., Lv, Y. S., Kang, W. W., and Zhao, Y. F.: A Deep Learning Based Approach for Traffic Data Imputation, IEEE 17th International Conference on Intelligent Transportation Systems (ITSC), Qingdao, PEOPLES R CHINA, Oct 08-11, WOS:000357868700163, 912-917, 10.1109/ITSC.2014.6957805, 2014.

Falge, E., Baldocchi, D., Olson, R., Anthoni, P., Aubinet, M., Bernhofer, C., Burba, G., Ceulemans, R., Clement, R., Dolman, H., Granier, A., Gross, P., Grunwald, T., Hollinger, D., Jensen, N. O., Katul, G., Keronen, P., Kowalski, A., Lai, C. T., Law, B. E., Meyers, T., Moncrieff, H., Moors, E., Munger, J. W., Pilegaard, K., Rannik, U., Rebmann, C., Suyker, A., Tenhunen,

https://doi.org/10.5194/egusphere-2023-2685
Preprint. Discussion started: 8 January 2024

J., Tu, K., Verma, S., Vesala, T., Wilson, K., and Wofsy, S.: Gap filling strategies for defensible annual sums of net ecosystem exchange, Agric. For. Meteorol., 107, 43-69, 10.1016/s0168-1923(00)00225-2, 2001.

Foltynova, L., Fischer, M., and McGloin, R. P.: Recommendations for gap-filling eddy covariance latent heat flux measurements using marginal distribution sampling, Theor. Appl. Climatol., 139, 677-688, 10.1007/s00704-019-02975-w, 2020.

Friedman, J., Hastie, J., and Tibshirani, R.: The elements of statistical learning, Springer, New York, NY, 10.1007/978-0-387-84858-7, 2009.

Gad, I., Hosahalli, D., Manjunatha, B. R., and Ghoneim, O. A.: A robust deep learning model for missing value imputation in big NCDC dataset, Iran Journal of Computer Science, 4, 67-84, 10.1007/s42044-020-00065-z, 2021.

Gao, Z., Chae, N., Kim, J., Hong, J., Choi, T., and Lee, H.: Modeling of surface energy partitioning, surface temperature, and soil wetness in the Tibetan prairie using the Simple Biosphere Model 2 (SiB2), 109, 10.1029/2003JD004089, 2004.

Goodfellow, I., Bengio, Y., Courville, A., and Bengio, Y.: Deep Learning (Vol. 1), The MIT Press, Cambridge, 10.1038/nature14539, 2016.

Hirsch, R. M., Slack, J. R., and Smith, R. A.: Techniques of trend analysis for monthly water quality data, Water Resour. Res., 18, 107-121, 10.1029/WR018i001p00107, 1982.

Hui, D. F., Wan, S. Q., Su, B., Katul, G., Monson, R., and Luo, Y. Q.: Gap-filling missing data in eddy covariance measurements using multiple imputation (MI) for annual estimations, Agric. For. Meteorol., 121, 93-111, 10.1016/s0168-1923(03)00158-8, 2004.

Jiao, B., Su, Y., Li, Q., Manara, V., and Wild, M.: An integrated and homogenized global surface solar radiation dataset and its reconstruction based on a convolutional neural network approach, Earth Syst. Sci. Data, 15, 4519-4535, 10.5194/essd-15-4519-2023, 2023.

Knox, S. H., Sturtevant, C., Matthes, J. H., Koteen, L., Verfaillie, J., and Baldocchi, D.: Agricultural peatland restoration: effects of land-use change on greenhouse gas (CO2 and CH4) fluxes in the Sacramento-San Joaquin Delta, Glob. Change Biol., 21, 750-765, 10.1111/gcb.12745, 2015.

Kohavi, R.: A study of cross-validation and bootstrap for accuracy estimation and model selection, Proceedings of the Fourteenth International Joint Conference on Artificial Intelligence, 1137-1143, 10.5555/1643031.1643047, 1995.

Krizhevsky, A., Sutskever, I., and Hinton, G.: ImageNet Classification with Deep Convolutional Neural Networks, Advances in neural information processing systems, 25, 1097-1105, 10.1145/3065386, 2012.

Lecun, Y., Bottou, L., Bengio, Y., and Haffner, P.: Gradient-based learning applied to document recognition, Proceedings of the Ieee, 86, 2278-2324, 10.1109/5.726791, 1998.

Lee, X., Massman, W. J., and Law, B. E.: Handbook of micrometeorology: a guide for surface flux measurement and analysis, 2004.

Li, C., He, H., Liu, M., Su, W., Fu, Y., Zhang, L., Wen, X., and Yu, G.: ChinaFLUX CO2 flux data processing system and its application, Journal of Geo-Information Science, 10, 557-565, 10.3969/j.issn.1560-8999.2008.05.002, 2008.

https://doi.org/10.5194/egusphere-2023-2685
Preprint. Discussion started: 8 January 2024

Little, R. J. A. and Rubin, D. B.: Statistical Analysis with Missing Data, Second Edition, John Wiley & Sons, Inc., Hoboken, New Jersey., 10.1002/9781119013563, 2002.

Ma, Y., Hu, Z., Xie, Z., Ma, W., Wang, B., Chen, X., Li, M., Zhong, L., Sun, F., Gu, L., Han, C., Zhang, L., Liu, X., Ding, Z., Sun, G., Wang, S., Wang, Y., and Wang, Z.: A long-term (2005–2016) dataset of hourly integrated land-atmosphere interaction observations on the Tibetan Plateau, Earth Syst. Sci. Data, 12, 2937-2957, 10.5194/essd-12-2937-2020, 2020.

Matusowsky, M., Ramotsoela, D. T., and Abu-Mahfouz, A. M.: Data Imputation in Wireless Sensor Networks Using a Machine Learning-Based Virtual Sensor, J. Sens. Actuar. Netw., 9, 25, 10.3390/jsan9020025, 2020.

Mauder, M., Foken, T., Clement, R., Elbers, J. A., Eugster, W., Grunwald, T., Heusinkveld, B., and Kolle, O.: Quality control of CarboEurope flux data - Part 2: Inter-comparison of eddy-covariance software, Biogeosciences, 5, 451-462, 10.5194/bg-5-451-2008, 2008.

Moffat, A. M., Papale, D., Reichstein, M., Hollinger, D. Y., Richardson, A. D., Barr, A. G., Beckstein, C., Braswell, B. H., Churkina, G., Desai, A. R., Falge, E., Gove, J. H., Heimann, M., Hui, D. F., Jarvis, A. J., Kattge, J., Noormets, A., and Stauch, V. J.: Comprehensive comparison of gap-filling techniques for eddy covariance net carbon fluxes, Agric. For. Meteorol., 147, 209-232, 10.1016/j.agrformet.2007.08.011, 2007.

Ooba, M., Hirano, T., Mogami, J. I., Hirata, R., and Fujinuma, Y.: Comparisons of gap-filling methods for carbon flux dataset: A combination of a genetic algorithm and an artificial neural network, Ecol. Model., 198, 473-486, 10.1016/j.ecolmodel.2006.06.006, 2006.

Ortega, L. C., Otero, L. D., Solomon, M., Otero, C. E., and Fabregas, A.: Deep learning models for visibility forecasting using climatological data, International Journal of Forecasting, 39, 992-1004, 10.1016/j.ijforecast.2022.03.009, 2023.

Papale, D., Reichstein, M., Aubinet, M., Canfora, E., Bernhofer, C., Kutsch, W., Longdoz, B., Rambal, S., Valentini, R., Vesala, T., and Yakir, D.: Towards a standardized processing of Net Ecosystem Exchange measured with eddy covariance technique: algorithms and uncertainty estimation, Biogeosciences, 3, 571-583, 10.5194/bg-3-571-2006, 2006.

Reichstein, M., Falge, E., Baldocchi, D., Papale, D., Aubinet, M., Berbigier, P., Bernhofer, C., Buchmann, N., Gilmanov, T., Granier, A., Grunwald, T., Havrankova, K., Ilvesniemi, H., Janous, D., Knohl, A., Laurila, T., Lohila, A., Loustau, D., Matteucci, G., Meyers, T., Miglietta, F., Ourcival, J. M., Pumpanen, J., Rambal, S., Rotenberg, E., Sanz, M., Tenhunen, J., Seufert, G., Vaccari, F., Vesala, T., Yakir, D., and Valentini, R.: On the separation of net ecosystem exchange into assimilation and ecosystem respiration: review and improved algorithm, Glob. Change Biol., 11, 1424-1439, 10.1111/j.1365-2486.2005.001002.x, 2005.

Shaoying, W., Yu, Z., Xianhong, M., Minhong, S., Lunyu, S., Youqi, S. U., and Zhaoguo, L. I.: Fill the Gaps of Eddy Covariance Fluxes Using Machine Learning Algorithms, Plateau Meteorology, 39, 1348-1360, 10.7522/j.issn.1000-0534.2019.00142, 2020.

Soloway, A. D., Amiro, B. D., Dunn, A. L., and Wofsy, S. C.: Carbon neutral or a sink? Uncertainty caused by gap-filling long-term flux measurements for an old-growth boreal black spruce forest, Agric. For. Meteorol., 233, 110-121, 10.1016/j.agrformet.2016.11.005, 2017.

https://doi.org/10.5194/egusphere-2023-2685
Preprint. Discussion started: 8 January 2024

Stull, R. B.: An Introduction to Boundary Layer Meteorology, Kluwer Academic Publishers Dordrecht., The Netherlands., 10.1007/978-94-009-3027-8, 1988.

Swinbank and W.C.: The measurement of vertical transfer of heat and water vapor by eddies in the lower atmosphere, Journal of Meteorology, 8, 135-145, 10.1175/1520-0469(1951)008<0135:TMOVTO>2.0.CO;2, 1951.

Vaswani, A., Shazeer, N., Parmar, N., Uszkoreit, J., Jones, L., Gomez, A. N., Kaiser, L., and Polosukhin, I.: Attention Is All You Need, 31st Annual Conference on Neural Information Processing Systems (NIPS), Long Beach, CA, Dec 04-09, WOS:000452649406008, 5998-6008, 10.5555/3295222.3295349, 2017.

Wang, S., Zhang, Y., Lv, S., Ao, Y., Li, S., and Chen, S.: Quality control research of turbulent data in Jinta oasis, Plateau Meteorology, 28, 1260-1273,ir.casnw.net/handle/362004/21874, 2009.

Wang, S., Zhang, Y., Meng, X., Song, M., Shang, L., Su, Y., and LI, Z.: Fill the Gaps of Eddy Covariance Fluxes Using Machine Learning Algorithms , Plateau Meteorology, 39, 1348-1360, 10.7522/j.issn.1000-0534.2019.00142, 2020.

Wutzler, T., Lucas-Moffat, A., Migliavacca, M., Knauer, J., Sickel, K., Sigut, L., Menzer, O., and Reichstein, M.: Basic and extensible post-processing of eddy covariance flux data with REddyProc, Biogeosciences, 15, 5015-5030, 10.5194/bg-15-5015-2018, 2018.

Yang, K., Wu, H., Qin, J., Lin, C. G., Tang, W. J., and Chen, Y. Y.: Recent climate changes over the Tibetan Plateau and their impacts on energy and water cycle: A review, Glob. Planet. Change, 112, 79-91, 10.1016/j.gloplacha.2013.12.001, 2014.

Yu, G., Chen, Z., Zhang, L., Peng, C., Chen, J., Pu, S., Zhang, Y., Niu, S., Wang, Q., Luo, Y., Ciais, P., and Baldocchi, D. D.: Re-recognizing the scientific mission of flux observation - Laying a solid data foundation for solving global sustainable development ecological issues, Journal of Resources and Ecology (English version), 8, 115-120, 10.5814/j.issn.1674-764x.2017.02.001, 2017.

Yue, S., Pilon, P., Phinney, B., and Cavadias, G.: The influence of autocorrelation on the ability to detect trend in hydrological series, Hydrological Processes, 16, 1807-1829, 10.1002/hyp.1095, 2002.

Zhang, C., Dazlich, D. A., Randall, D. A., Sellers, P. J., and Denning, A. S.: Calculation of the global land surface energy, water and CO2 fluxes with an off-line version of SiB2, 101, 19061-19075, 10.1029/96JD01449, 1996.

Zheng, D., Zhang, Q. s., and Wu, S.: Mountain Geoecology and Sustainable Development of the Tibetan Plateau, Kluwer Academic, Dordrecht, the Netherlands, 10.1007/978-94-010-0965-2, 2000.